# Positive Supercoiling of Mitotic DNA Drives Decatenation by Topoisomerase II in Eukaryotes

J. Baxter, *et al.*

*Science* **331**, 1328 (2011);
DOI: 10.1126/science.1201538

intense male-male competition for mates, males and females showed significant differences in either *IMR* or *RoA*, and male life span was shorter than female life span (baboons, sifaka, gorillas, chimpanzees, and capuchins; we lacked mortality data for male blue monkeys; see Fig. 1 and table S3). In contrast, male and female muriquis were indistinguishable in their *IMR*s, *RoA*s, and life spans (table S3). This male-female similarity in muriqui aging patterns, combined with the observation of multiple mating by both sexes in all of our study species, suggests that the male-male competitive environment, not just multiple mating by males, may be a key factor driving faster aging in males in polygynandrous species [see also (*26*)].

If demographic patterns of aging were evolutionarily constrained, we would expect closely related species of primates to exhibit similar aging patterns. Instead, the species rankings of *IMR* and *RoA* in males and females showed no relationship to phylogeny (Fig. 2C and fig. S1). This implies that the study species have not been constrained phylogenetically to high or low aging rates, and have the flexibility to respond to evolutionary forces at the species level or potentially even the local population level. Furthermore, within-species comparisons of baboons (*31*), chimpanzees (*23*, *32*), and humans (*23*, *25*) all support the view that both *IMR* and *RoA* can vary substantially among populations within a species. Notably, in all three species, populations existing in more demanding habitats, without benefit of modern medical intervention (e.g., hunter-forager humans and wild as opposed to captive primates), exhibit higher *IMR* and, for both chimpanzees and humans, higher *RoA*. That is, aging appears to be both evolutionarily labile and phenotypically plastic. The slowing of aging-related disease under dietary restriction (*33*) is further evidence of the flexibility of aging rates in primates.

We examined our data for the existence of mortality plateaus (*34*), a subject of much recent interest in the aging literature, but none of the age-specific mortality relationships in our nonhuman primate analyses demonstrated the type of leveling off that has been shown in human and fly data sets [e.g., (*35*)]. Whether additional long-term data from natural primate populations will demonstrate a generalized mortality deceleration in old age remains an open question that should motivate future comparative analyses of aging in other natural populations.


**References and Notes**

1. C. E. Finch, M. C. Pike, M. Witten, *Science* **249**, 902 (1990).
2. R. E. Ricklefs, *Proc. Natl. Acad. Sci. U.S.A.* **107**, 10314 (2010).
3. C. Finch, *Longevity, Senescence and the Genome* (Univ. of Chicago Press, Chicago, 1990).
4. G. A. Sacher, in *Handbook of the Biology of Aging*, C. E. Finch, L. Hayflick, Eds. (Van Nostrand Reinhold, New York, 1977), pp. 582–638.
5. W. C. Sanderson, S. Scherbov, *Science* **329**, 1287 (2010).
6. W. Lutz, W. Sanderson, S. Scherbov, *Nature* **451**, 716 (2008).
7. N. S. Gavrilova *et al.*, *Hum. Biol.* **70**, 799 (1998).
8. J. Evert, E. Lawler, H. Bogan, T. Perls, *J. Gerontol. A Biol. Sci. Med. Sci.* **58**, 232 (2003).
9. R. G. J. Westendorp, T. B. L. Kirkwood, *Nature* **396**, 743 (1998).
10. T. B. L. Kirkwood, *Nature* **451**, 644 (2008).
11. A. K. Brunet-Rossinni, S. N. Austad, in *Handbook of the Biology of Aging*, E. J. Masoro, S. N. Austad, Eds. (Elsevier, Amsterdam, 2006), pp. 243–266.
12. T. Clutton-Brock, B. C. Sheldon, *Science* **327**, 1207 (2010).
13. W. F. Morris *et al.*, *Am. Nat.* **177**, E14 (2011).
14. K. B. Strier *et al.*, *Methods Ecol. Evol.* **1**, 199 (2010).
15. Supporting material is provided on *Science* Online.
16. E. Arias, *United States life tables, 2004*. National Vital Statistics Reports (National Center for Health Statistics, Hyattsville, MD, 2007), vol. 56.
17. R. N. Anderson, *United States life tables, 1997*. National Vital Statistics Reports (National Center for Health Statistics, Hyattsville, MD, 1999), vol. 47.
18. K. W. Wachter, *Popul. Dev. Rev.* **29** (suppl.), 270 (2003).
19. K. W. Wachter, C. E. Finch, Eds., *Between Zeus and the Salmon: The Biodemography of Longevity* (National Academy Press, Washington, DC, 1997).
20. S. D. Pletcher, *J. Evol. Biol.* **12**, 430 (1999).
21. A. M. Bronikowski, D. E. L. Promislow, *Trends Ecol. Evol.* **20**, 271 (2005).
22. T. B. Gage, *Annu. Rev. Anthropol.* **27**, 197 (1998).
23. K. Hawkes, K. R. Smith, S. L. Robson, *Am. J. Hum. Biol.* **21**, 578 (2009).
24. D. E. L. Promislow, M. Tatar, A. A. Khazaeli, J. W. Curtsinger, *Genetics* **143**, 839 (1996).
25. M. Gurven, H. Kaplan, *Popul. Dev. Rev.* **33**, 321 (2007).
26. T. H. Clutton-Brock, K. Isvaran, *Proc. Biol. Sci.* **274**, 3097 (2007).
27. J. Allman, A. Rosin, R. Kumar, A. Hasenstaub, *Proc. Natl. Acad. Sci. U.S.A.* **95**, 6866 (1998).
28. J. C. Mitani, J. Gros-Louis, A. F. Richard, *Am. Nat.* **147**, 966 (1996).
29. R. R. Lawler, A. F. Richard, M. A. Riley, *J. Hum. Evol.* **48**, 259 (2005).
30. K. B. Strier, *Behaviour* **130**, 151 (1994).
31. A. M. Bronikowski *et al.*, *Proc. Natl. Acad. Sci. U.S.A.* **99**, 9591 (2002).
32. K. Hill *et al.*, *J. Hum. Evol.* **40**, 437 (2001).
33. R. J. Colman *et al.*, *Science* **325**, 201 (2009).
34. J. W. Vaupel *et al.*, *Science* **280**, 855 (1998).
35. R. Rau, E. Soroko, D. Jasilionis, J. W. Vaupel, *Popul. Dev. Rev.* **34**, 747 (2008).


36. The National Evolutionary Synthesis Center (NESCent) and the National Center for Ecological Analysis and Synthesis (NCEAS) jointly supported the Primate Life Histories Working Group. H. Lapp and X. Liu at NESCent provided expert assistance in designing and implementing the Primate Life Histories Database (PLHD). J. Moorad commented on the manuscript. The governments of Brazil, Costa Rica, Kenya, Madagascar, Rwanda, and Tanzania provided permission for our field studies, and all research complied with guidelines in the host countries. For study-specific acknowledgments and Institutional Animal Care and Use Committee compliance, see http://demo.plhdb.org. The nonhuman primate data used in these analyses are available in the Dryad database (http://dx.doi.org/10.5061/dryad.8682).


**Supporting Online Material**

www.sciencemag.org/cgi/content/full/331/6022/1325/DC1
Methods
Figs. S1 to S8
Tables S1 to S10
References


13 December 2010; accepted 1 February 2011
10.1126/science.1201571


# Positive Supercoiling of Mitotic DNA Drives Decatenation by Topoisomerase II in Eukaryotes


**J. Baxter,[1,4]* N. Sen,[1]† V. López Martínez,[2]† M. E. Monturus De Carandini,[2]† J. B. Schvartzman,[2] J. F. X. Diffley,[3] L. Aragón[1]***



**DNA topoisomerase II completely removes DNA intertwining, or catenation, between sister chromatids before they are segregated during cell division. How this occurs throughout the genome is poorly understood. We demonstrate that in yeast, centromeric plasmids undergo a dramatic change in their topology as the cells pass through mitosis. This change is characterized by positive supercoiling of the DNA and requires mitotic spindles and the condensin factor Smc2. When mitotic positive supercoiling occurs on decatenated DNA, it is rapidly relaxed by topoisomerase II. However, when positive supercoiling takes place in catenated plasmid, topoisomerase II activity is directed toward decatenation of the molecules before relaxation. Thus, a topological change on DNA drives topoisomerase II to decatenate molecules during mitosis, potentially driving the full decatenation of the genome.**


In eukaryotes, most topological links between the DNA strands are removed during DNA replication by topoisomerases I and II (fig. S1A) (*1*). However, many links are converted into double-stranded DNA intertwines or catenanes during the completion of replication (*2*, *3*). These can only be resolved by topoisomerase II (fig. S1) (*4*).

Passage through mitosis is required for complete decatenation, because topoisomerase II activity is essential during mitosis as late as anaphase (fig. S1B) (*4*–*6*). Because mitotic spindles are required to complete decatenation, it is assumed to occur only after chromosome segregation during anaphase (*4*). However, sister chromatids appear to be fully decatenated before their physical separation by spindles (*7*, *8*). Potential alternate mechanisms, in which decatenation is promoted by supercoiling, have been proposed in prokaryotes (*9*–*11*). These mechanisms prompted us to study whether mitotic changes to DNA topology help drive decatenation in eukaryotes.

We assayed in vivo DNA topology with circular plasmids, which retain topological information after DNA extraction (*12*). We used yeast plasmids that contain yeast-origin and centromeric sequences whose segregation behavior generally mimics that of endogenous chromosomes. However, these small plasmids are mostly decatenated shortly after DNA replication in the presence of wild-type (WT) levels of topoisomerase II (Fig. 1A). Therefore, we used the top2-td degron strain (*6*) to ensure an enriched population of catenated DNA that could be examined through the later stages of the cell cycle. Passage through DNA replication in the absence of topoisomerase II converted the supercoiled monomer pRS316 plasmid (CCCm) into catenated plasmid dimer (CatC). Both CCCm and CatC were negatively supercoiled, consistent with normal chromatinization (*6*).

Assaying the electrophoretic mobility of these plasmids throughout the rest of the cell cycle showed that their mobility changed significantly between 40 and 80 min as the cells started entering anaphase (Fig. 1A). Chloroquine intercalation confirmed that the catenated plasmids were still composed of intact plasmids (fig. S2), and in vitro topoisomerase Ib treatment confirmed that the catenated plasmids were topoisomers of the CatC dimers that formed after replication (fig. S6A). We refer to the premitotic form as C-type catenanes (CatC) and to the mitotic form as C*-type catenanes (CatC*).

The transition from CatC to CatC* coincided with chromosome segregation. In cells arrested in metaphase by depletion of the anaphase-promoting–complex activator Cdc20 (*top2-td cdc20-td*), we observed the CatC-to-CatC* transition, which indicates that it occurred before anaphase onset (Fig. 1B). We detected CatC* dimers until cells exited mitosis (fig. S3), demonstrating that the CatC* catenanes occur when both mitotic cyclin-dependent kinases are active and mitotic spindles are present. However, CatC* dimer formation did not take place in cells arrested in metaphase with the microtubule-depolymerizing drug nocodazole

[1]Cell Cycle Group, Medical Research Council (MRC) Clinical Sciences Centre, Imperial College London, Hammersmith Hospital, Du Cane Road, London W12 0NN, UK. [2]Department of Cell Proliferation and Development, Centro de Investigaciones Biológicas (CSIC), Ramiro de Maeztu 9, 28040 Madrid, Spain. [3]Clare Hall Laboratories, Cancer Research UK London Research Institute, South Mimms EN6 3LD, UK. [4]Genome Damage and Stability Centre, Science Park Road, University of Sussex, Falmer, Brighton, East Sussex BN1 9RQ, UK.

*To whom correspondence should be addressed. E-mail: luis.aragon@csc.mrc.ac.uk (L.A.); Jon.Baxter@sussex.ac.uk (J.B.)

†These authors contributed equally to this work.

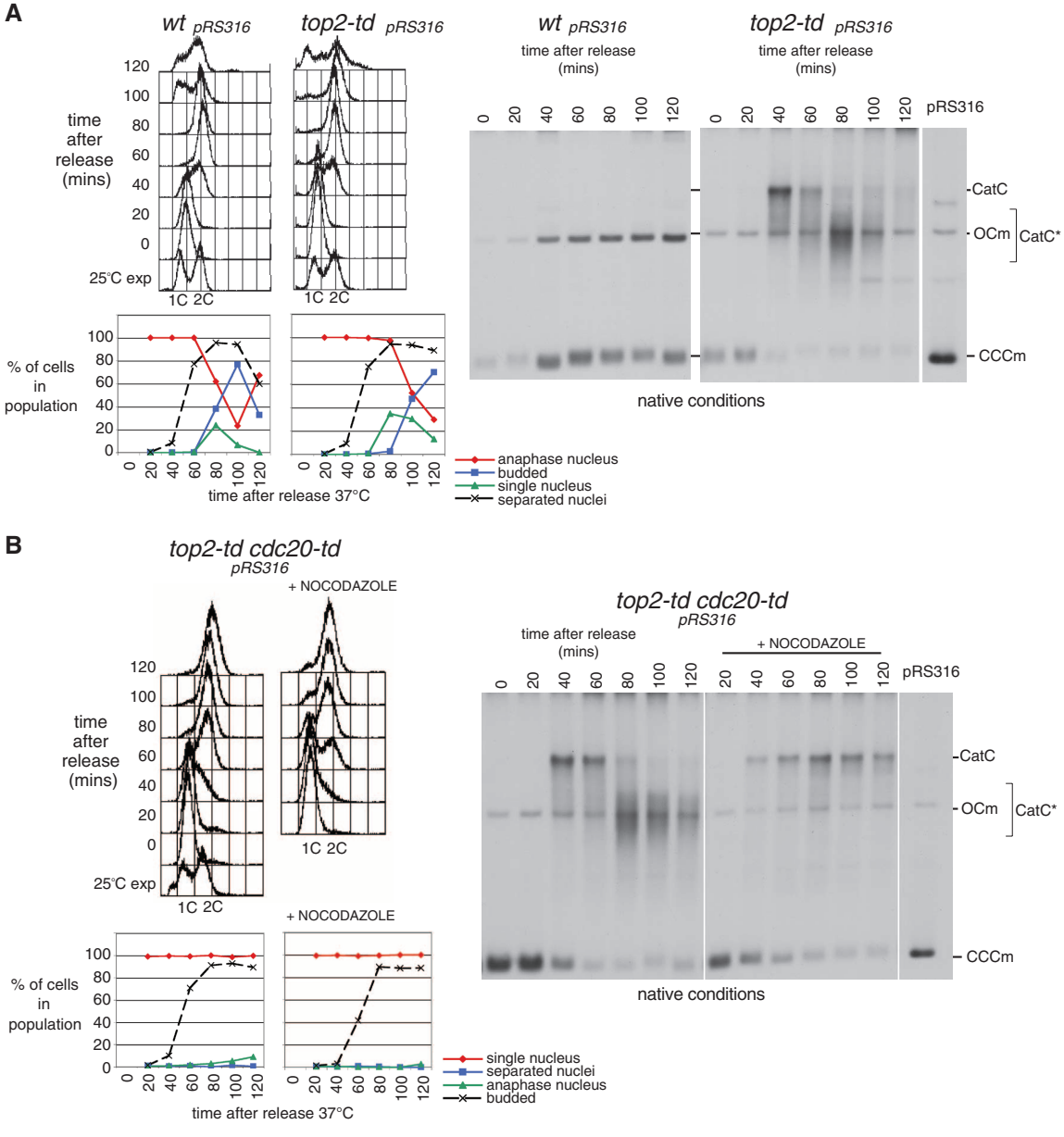


**Fig. 1.** Mitosis and spindle formation induce a topological change in catenated plasmid DNA in vivo. (**A**) WT pRS316 and top2-td pRS316 cells were synchronized in $G_1$ and top2-td-depleted of Top2. The cells were synchronously released into the cell cycle, and regular samples were taken for analysis. (Histograms at left) Fluorescence-activated cell sorting analysis of DNA content and the histogram of kinetics of nuclear division and budding index. (Right panel) Autoradiogram of a blot containing cellular DNA electrophoretically resolved in agarose and probed for pRS316 sequences. Electrophoretic mobilities of CCCm (covalently closed circular monomers), OCm (open circle monomers), and CatC (covalently closed catenated dimers) are indicated. The region where the topologically modified CatC-CatC* resolve is also indicated. (**B**) Double degron cdc20-td top2-td pRS316 strains were processed as in (A), but were arrested before anaphase entry by either depletion of Cdc20 or treatment with nocodazole, in addition to Cdc20 depletion.

(Fig. 1B). Therefore, mitotic spindles are required for the transition from CatC to CatC*. The noncentromeric plasmid pRS426 did not undergo the distinct transition to CatC* in the absence of Top2 (fig. S4), suggesting that spindles must be engaged with kinetochores in cis for the transition to occur.

The CatC-to-CatC* transition was not due to residual Top2 decatenation activity in mitosis, because in vitro nicking of the two types of catenated dimers generated very similar populations of relaxed catenanes (fig. S5), indicative of similar catenation states.

To examine whether the CatC-to-CatC* transition correlated with any changes in supercoiling, we treated DNA samples enriched for either of the catenated dimers (CatC enriched by nocodazole arrest and CatC* enriched by cdc20 arrest) with eukaryotic topoisomerase I (topo IB), which relaxes both negative and positive supercoils, or *Escherichia coli* topoisomerase I (topo IA), which relaxes only negative supercoils. Topo IB relaxed catenated dimers from both CatC and CatC* samples (fig. S6A). However, topo IA relaxed CatC but not CatC* catenanes (Fig. 2A and fig. S6A), indicating that the intertwined plasmids in CatC* dimers are positively supercoiled, whereas those in CatC are negatively supercoiled.

We used both titration analysis (Fig. 2B) and high-resolution analysis of partially nicked catenanes (fig. S6B) to confirm this finding by demonstrating that CatC dimers responded to chloroquine intercalation as if negatively supercoiled, whereas CatC* dimers responded as if positively supercoiled. Thus, the CatC-to-CatC* transition induced by mitotic spindles is due to a change from negative supercoiling (in CatC) to positive supercoiling (in CatC*).

Because the plasmids enter mitosis in a highly catenated state (due to topoisomerase II depletion), it is possible that positive supercoiling only occurs in this experimental situation. Therefore, we analyzed the supercoiling of plasmids that were decatenated by topoisomerase II immediately after DNA replication in both the absence and presence of mitotic spindles. Cells were allowed to replicate their DNA in the presence of Top2 activity before being arrested in metaphase by nocodazole treatment. Cdc20 was depleted to prevent entry into anaphase, and nocodazole was washed off to allow mitotic spindles to form. DNA was isolated from cells in nocodazole [without spindles] and from cells after the wash-off of nocodazole [with spindles], and the supercoiling of monomer plasmids was compared. Spindle formation shifted the supercoiling distribution to a more positive state (Fig. 2C, top panel). However, the extent of positive supercoiling appeared minor compared with the increase in positive supercoiling previously observed in catenated dimers generated in the absence of Top2 (Fig. 2B and fig. S6B). Normally, in vivo topoisomerases are extremely efficient in relaxing DNA topological perturbations. But depletion of topoisomerase II, which is used to generate catenated DNA, will also reduce the supercoiling relaxation activity of the cell. This could possibly stabilize induced positive supercoiling, promoting its detection in top2 depleted cells. To investigate this, we repeated the experiment but depleted Top2 specifically during the period when mitotic spindles were reformed. We then observed that a substantial proportion of the negatively supercoiled monomer plasmids observed in nocodazole became highly positively supercoiled when spindles formed (Fig. 2C, bottom panel). Therefore, a potent positive supercoiling activity is induced on both decatenated-monomer (Fig. 2C) and catenated-dimer plasmids (Fig. 2, A and B, and fig. S6) during mitosis. However, the induced positive supercoiling is normally rapidly relaxed by topoisomerase II (Fig. 2C).

Mitotic spindles are required to complete topoisomerase II–mediated decatenation of chromosomes during mitosis (*4*, *5*). Here, we demonstrate that in mitosis, spindles induce a potent positive supercoiling activity on plasmid DNA. In prokaryotes, intrachromosomal supercoiling promotes decatenation (*9*–*11*). Therefore, the mitotic positive supercoiling activity could be required to promote decatenation by topoisomerase II. We treated DNA enriched for either the nega-

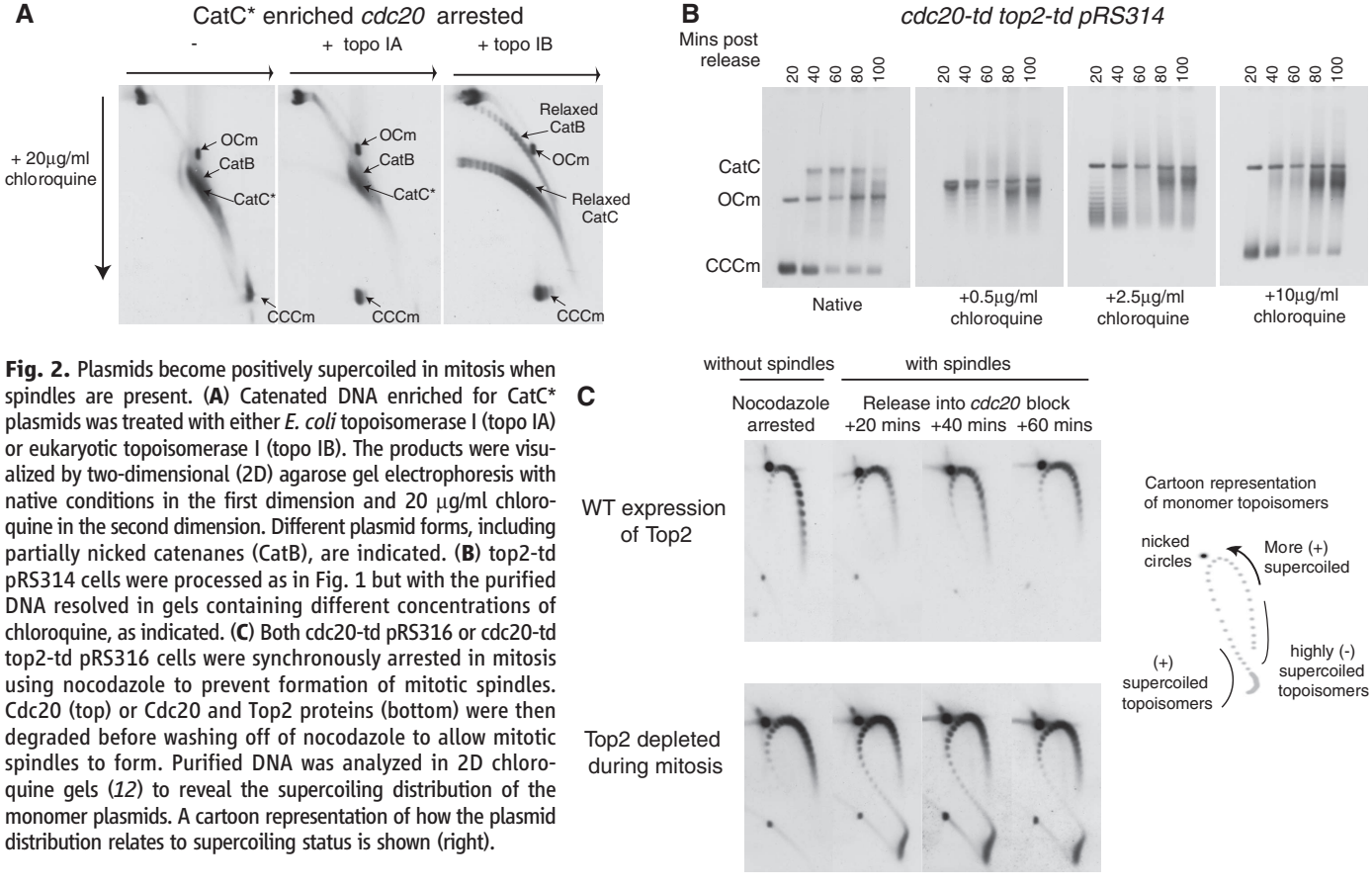


**Fig. 2.** Plasmids become positively supercoiled in mitosis when spindles are present. (**A**) Catenated DNA enriched for CatC* plasmids was treated with either *E. coli* topoisomerase I (topo IA) or eukaryotic topoisomerase I (topo IB). The products were visualized by two-dimensional (2D) agarose gel electrophoresis with native conditions in the first dimension and 20 µg/ml chloroquine in the second dimension. Different plasmid forms, including partially nicked catenanes (CatB), are indicated. (**B**) top2-td pRS314 cells were processed as in Fig. 1 but with the purified DNA resolved in gels containing different concentrations of chloroquine, as indicated. (**C**) Both cdc20-td pRS316 or cdc20-td top2-td pRS316 cells were synchronously arrested in mitosis using nocodazole to prevent formation of mitotic spindles. Cdc20 (top) or Cdc20 and Top2 proteins (bottom) were then degraded before washing off of nocodazole to allow mitotic spindles to form. Purified DNA was analyzed in 2D chloroquine gels (*12*) to reveal the supercoiling distribution of the monomer plasmids. A cartoon representation of how the plasmid distribution relates to supercoiling status is shown (right).

tively supercoiled CatC dimers or the positively supercoiled CatC* dimers with different amounts of recombinant topoisomerase II. Topoisomerase II treatment of CatC dimers (nocodazole-arrested) initially produced catenanes with progressively slower electrophoretic mobilities. Resolved monomers were only observed at relatively high enzyme concentrations (>20 units) (Fig. 3, A and C). The kinetics that we observed are consistent with topoisomerase II concurrently relaxing negative supercoils and decatenating the interplasmid links in CatC dimers, so that when the final catenanes are resolved, only a small number of supercoils remain on the monomer plasmids. In contrast, the positively supercoiled CatC* plasmids (cdc20-arrested) were fully decatenated at the lowest topoisomerase II concentration tested (Fig. 3A). Decatenation of the CatC* dimers required one order of magnitude fewer units of enzyme (Fig. 3, B and D). The CatC* catenanes were resolved directly into highly supercoiled monomers at low topoisomerase concentrations, and we observed relaxation of the resultant supercoiled monomers only after complete decatenation (Fig. 3B). Therefore, although positive supercoiling of decatenated monomer plasmids is rapidly followed by topoisomerase II relaxation, induction of positive supercoiling on catenated plasmids drives topoisomerase II to resolve any intermolecular catenated links before positive-supercoil relaxation.

We surmised that kinetochore attachment may indirectly induce topological change through activation of centromere-associated complexes that can modulate DNA topology. One such candidate complex is the condensin SMC2/4 complex (*13*, *14*). We asked whether SMC2 activity was required for the positive supercoiling that characterizes CatC* by assessing whether the transition from CatC to CatC* occurs in the condensin smc2-8 mutant background (*15*). DNA replication in the absence of SMC2 and TOP2 function generated significant levels of CatC dimers (Fig. 4A). However, no transition from CatC to CatC* could be observed (Fig. 4A), despite the normal formation of mitotic spindles in this background (fig. S7). Furthermore, Smc2 function was required for the positive supercoiling of decatenated monomer plasmids. Formation of mitotic spindles in the top2-td strain with WT Smc2 function generated high levels of positive supercoiling in the monomer plasmids (Fig. 4B, left panel). However, positively supercoiled plasmids could not be observed when Smc2 function was disrupted (Fig. 4B, middle panel). The absence of positively supercoiled monomers was not due to a lack of functional spindles, because both the smc2-8 top2-td and top2-td cells had similar numbers of cells undergoing anaphase and nuclear segregation after formation of mitotic spindles (Fig. 4B, right panels). Thus, we conclude that Smc2 function is required for the mitotic positive-supercoiling activity.



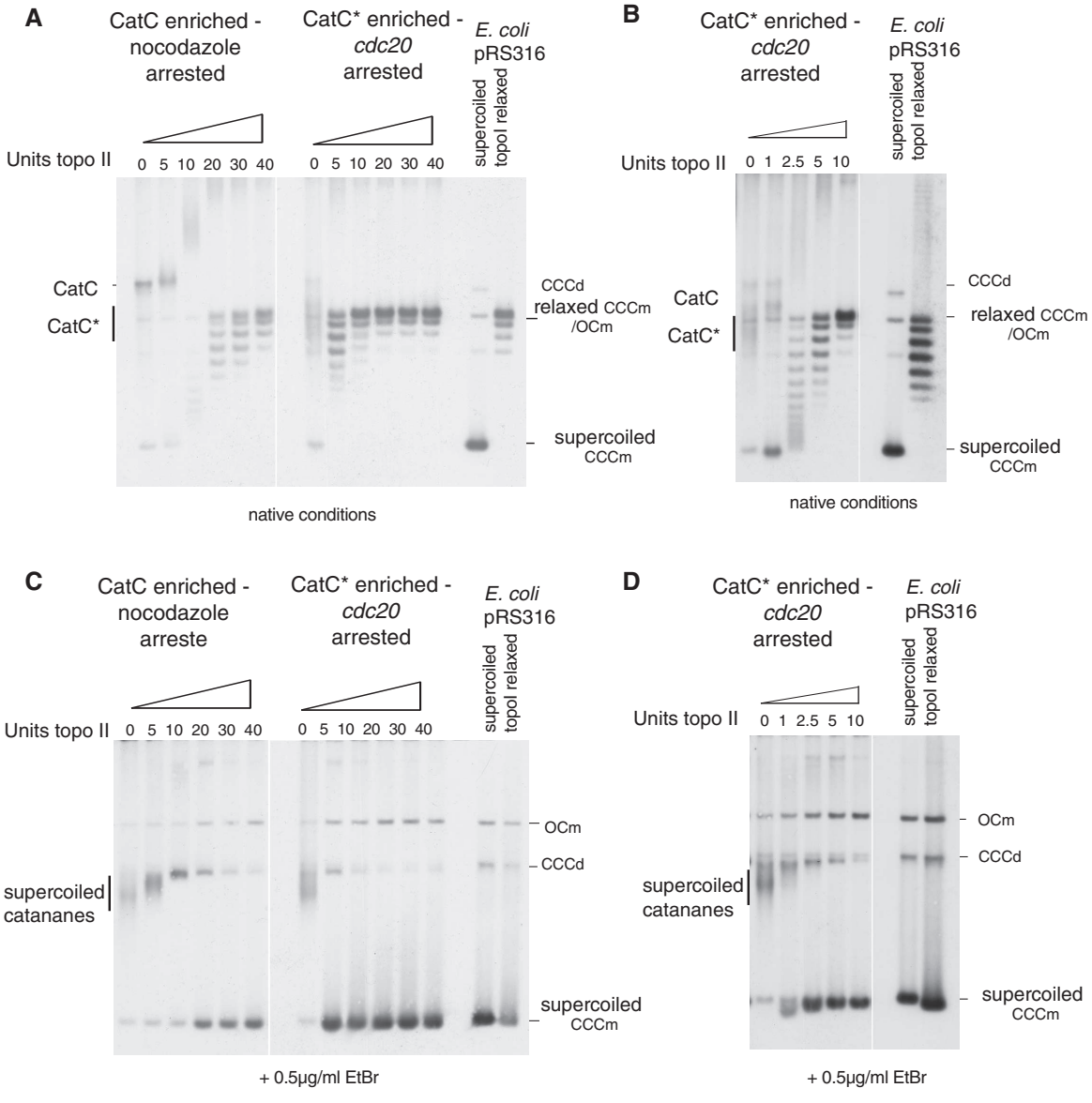


**Fig. 3.** CatC* catenated plasmids are preferentially decatenated by topoisomerase II in vitro. Catenated DNA enriched for CatC plasmids (nocodazole-arrested) or catenated DNA enriched for CatC* plasmids (cdc20-arrested) was treated in vitro with recombinant topoisomerase IIα, and the products were analyzed on agarose gels. Autoradiograms of blots where the DNA was treated with 5 to 40 units [(**A**) and (**C**)] or 1 to 10 units of enzyme [(**B**) and (**D**)] are shown. Products were resolved in either native agarose [(A) and (B)] or agarose containing 0.5 μg/ml EtBr [(C) and (D)] to confirm that plasmids remained covalently closed during treatment. $5 \times 10^{-9}$ grams of purified (*E. coli*) supercoiled and relaxed (topo I–treated) pRS316 was also resolved on each gel.

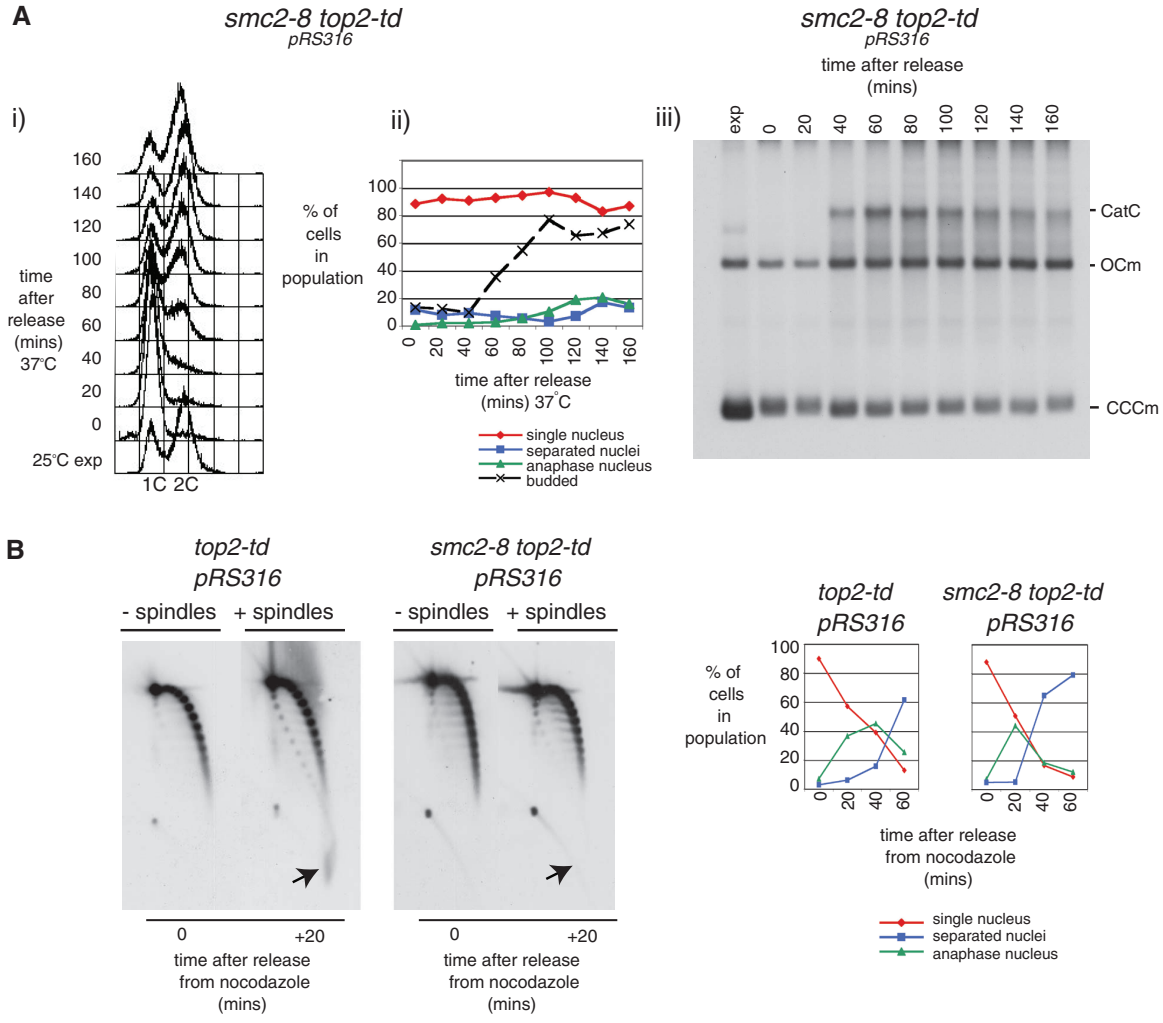


**Fig. 4.** Condensin SMC2 is required to positively supercoil plasmids during mitosis. (**A**) smc2-8 top2-td pRS316 cells were processed as in Fig. 1 to assess the electrophoretic mobility of the plasmid after disruption of both SMC2 and TOP2 functions. (**B**) top2-td and smc2-8 top2-td cells were processed as in Fig. 2C to specifically disrupt TOP2 and SMC2 during the period when mitotic spindles were formed in the cells after washing off of nocodazole and anaphase entry. (Left) Autoradiograms of plasmid supercoiling in nocodazole and 20 min after washing off are shown. Highly positively supercoiled monomers are indicated by arrows. (Right) Histogram indicating nuclear morphology of cells before and after nocodazole wash-off is shown.

Extrapolating from our data and previously proposed hypothetical models (*10*, *16*) of how SMC-mediated compaction may facilitate chromosome decatenation, we propose a model for how complete decatenation of the genome by topoisomerase II is accomplished during mitosis (outlined in fig. S8). Although Top2 can actively remove catenations between sister chromatids postreplication, residual catenanes are present at the time of mitosis (hence, the observed requirement for Top2 at this stage of the cell cycle). We propose that extensive positive supercoiling induced by mitotic spindles and condensin generates a topology on catenated chromosomes where intermolecular crossovers are isolated from intramolecular crossovers with a geometry that maximizes topoisomerase II decatenation activity. Once the sister chromatids are fully decatenated, topoisomerase II rapidly relaxes the positive supercoiling generated, returning the intrachromosomal topology of the sister chromatids to a state comparable to that observed before the transition, except that now, crucially, all catenated links have been removed.

### References and Notes


1. J. C. Wang, *Nat. Rev. Mol. Cell Biol.* **3**, 430 (2002).
2. O. Sundin, A. Varshavsky, *Cell* **21**, 103 (1980).
3. O. Sundin, A. Varshavsky, *Cell* **25**, 659 (1981).
4. C. Holm, T. Goto, J. C. Wang, D. Botstein, *Cell* **41**, 553 (1985).
5. T. Uemura *et al.*, *Cell* **50**, 917 (1987).
6. J. Baxter, J. F. Diffley, *Mol. Cell* **30**, 790 (2008).
7. R. A. Oliveira, R. S. Hamilton, A. Pauli, I. Davis, K. Nasmyth, *Nat. Cell Biol.* **12**, 185 (2010).
8. F. Uhlmann, D. Wernic, M. A. Poupart, E. V. Koonin, K. Nasmyth, *Cell* **103**, 375 (2000).
9. E. L. Zechiedrich, A. B. Khodursky, N. R. Cozzarelli, *Genes Dev.* **11**, 2580 (1997).
10. C. D. Hardy, N. J. Crisona, M. D. Stone, N. R. Cozzarelli, *Philos. Trans. R. Soc. London Ser. B Biol. Sci.* **359**, 39 (2004).
11. M. L. Martínez-Robles *et al.*, *Nucleic Acids Res.* **37**, 5126 (2009).
12. Materials and methods are available as supporting material on *Science* Online.
13. K. Kimura, M. Hirano, R. Kobayashi, T. Hirano, *Science* **282**, 487 (1998).
14. J. St-Pierre *et al.*, *Mol. Cell* **34**, 416 (2009).
15. L. Freeman, L. Aragon-Alcaide, A. Strunnikov, *J. Cell Biol.* **149**, 811 (2000).
16. T. Hirano, *Annu. Rev. Biochem.* **69**, 115 (2000).


17. We thank members of the Aragon laboratory, M. Merkenschlager, A. Carr, and J. Murray for discussions and critical reading of the manuscript. We also thank K. Nasmyth and S. Henikoff for helpful discussions, as well as anonymous referees for useful suggestions. This work was funded by European Research Council starting grant 202337 (L.A. and J.B.), the Royal Society (J.B.), the Spanish government grant BFU2008-00408/BMC (J.B.S.), Cancer Research UK (J.F.X.D.), and the MRC UK (L.A.). Extended figure legends are available in the supporting online material.


### Supporting Online Material

www.sciencemag.org/cgi/content/full/331/6022/1328/DC1
Materials and Methods
SOM Text
Figs. S1 to S8
Table S1
References

10 December 2010; accepted 28 January 2011
10.1126/science.1201538